Flow Separation near the Crests of Short Gravity Waves

MICHAEL S. LONGUET-HIGGINS

Center for Studies of Nonlinear Dynamics, La Jolla Institute, La Jolla, California and Department of Applied Mathematics and Theoretical Physics, Cambridge, England

27 July 1989 and 18 October 1989

ABSTRACT

Laboratory observations of short gravity waves of length about 1 m by Koga show the occurrence of a downward flow separation near the wave crests, making angles of 10° to 50° with the horizontal. Koga's observations are compared with a theoretical model of flow separation suggested by Longuet-Higgins. Some features of agreement are found.

1. Introduction

Steep surface waves in deep water are known to become unstable in a variety of ways, some of which have been described in a recent review (Longuet-Higgins 1987). Among the better known instabilities is the *whitecap,* or bubbly roller, which develops on the forward face of a progressive gravity wave having a wavelength greater than a few meters. A theoretical model for this flow was proposed by Longuet-Higgins and Turner (1974). At much shorter wavelengths, less than about 10 cm, capillary–gravity waves can trap pockets of air in the wave troughs, as first suggested by Crapper (1957) and observed experimentally by Toba (1961). However, at intermediate length-scales, of the order 1 m, a different type of instability has been observed by Koga (1982). It is this that we wish to discuss in the following note.

Koga (1982) found that near the crest of a steep gravity wave having a period of about 0.73 s (wavelength 75 cm), a structured flow could be observed. A cluster of bubbles was carried downwards into the interior of the fluid at an angle of about 40° to the horizontal (see Fig. 1a). Sometimes several such bubble clusters were visible, as in Figs. 1b and 1c. The flow appeared to separate from the free surface along a line which marked the boundary between relatively smooth flow ahead, (i.e. downwind) of the separation line, and a rough, apparently turbulent region behind (i.e., upwind) of the line. The separation was confirmed by photographs of the surface taken from below and pointing vertically upwards (Koga 1982, Fig. 5). The measured velocities in the bubble sheets, including their directions, are shown in Fig. 2 (adapted from Koga 1982).

The phenomenon is comparable to, but different from, the flow studied by Banner and Phillips (1974). They observed the separation at the edge of a turbulent roller artificially induced by placing a submerged obstacle in a steady current. In that case the angle of depression of the separated flow appears to be somewhat smaller, and the flow resembles more the flow beneath a whitecap.

Returning to Koga's observations, we emphasise that such a separated flow, involving as it sometimes does the entrainment of air bubbles, is of considerable interest in connection with the production of underwater sound at low wind speeds. Although the turbulent zone upwind of the line of separation may not be as easily visible from above as in a whitecap, nevertheless the process of trapping of air pockets, and their subsequent distortion into spherical bubbles, can be expected to contribute significantly to the level of underwater sound (Longuet-Higgins 1989a,b).

In the present note we draw attention to the fact that several years before Koga's (1982) paper, a theoretical model for the separation of flow at a free surface was suggested by Longuet-Higgins (1973). The model, in its simplest form, has several features corresponding closely with Koga's observations. In section 2 we outline the main features of the model, and in section 3 we shall compare it with Koga's observations. A discussion follows in section 4 and conclusions in section 5.

2. A theoretical model

The model is sketched in Fig. 3. In the unshaded region to the right, bounded by the free surface $\theta = \alpha$ and the sloping plane $\theta = -\beta$, the flow is assumed to be inviscid and irrotational. The density ρ in this region

Corresponding author address: Dr. Michael S. Longuet-Higgins, La Jolla Institute, 7855 Fay Avenue, Suite 300, P.O. Box 1434, La Jolla, CA 92038.

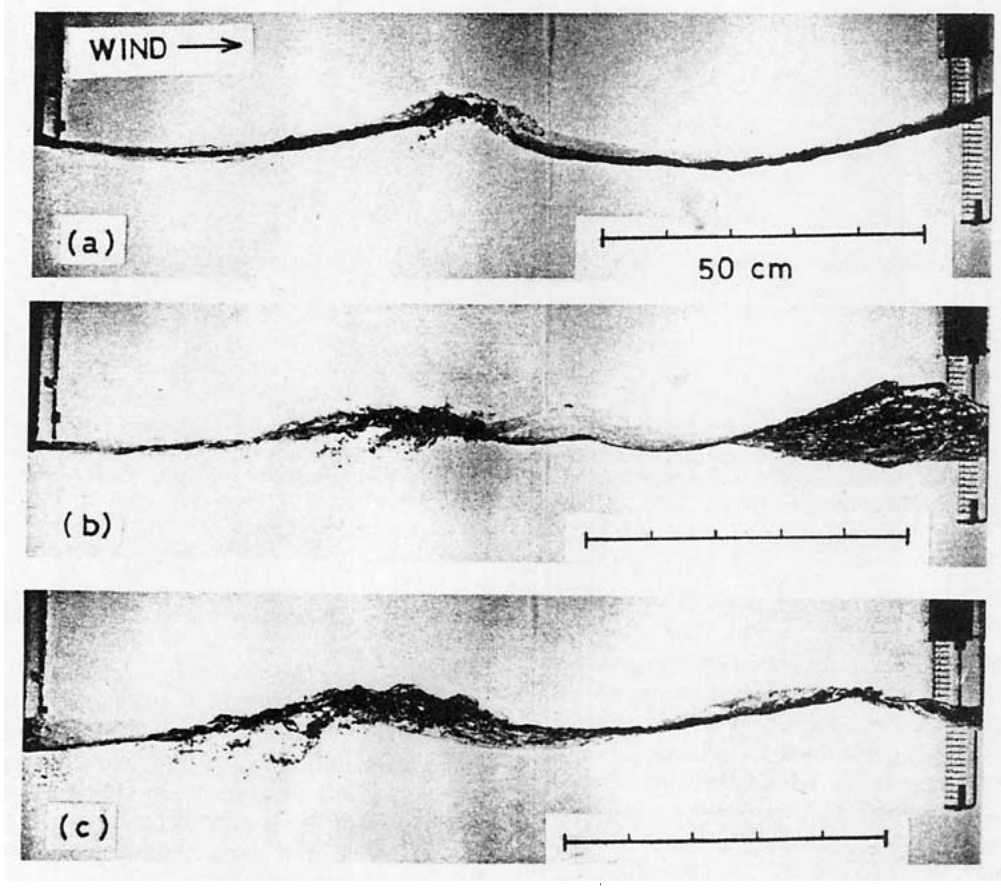

FIG. 1. Entrainment of bubble clusters in breaking wind waves. Wind-speed 16 m s^{-1}. Fetch 16.4 m. (From Koga 1982).

is assumed constant. To satisfy both Laplace's equation and the condition of constant pressure when $\theta = \alpha$ we take as streamfunction

$$\psi = Ar^{3/2} \sin \tfrac{3}{2}(\theta - \alpha) \tag{2.1}$$

where

$$A^2 = \tfrac{8}{9} g \cos\alpha. \tag{2.2}$$

(The case $\alpha = \frac{1}{3}\pi$ corresponds to Stokes' well-known corner flow). The pressure p and the velocity q are then given by

$$\frac{p}{\rho} = gr\cos\theta - \tfrac{1}{2} q^2 \tag{2.3}$$

$$q^2 = \tfrac{9}{4} A^2 r. \tag{2.4}$$

It will be seen that both p and q are proportional to the radial distance r. There is a stagnation point at $r = 0$.

In the shaded region to the left, where $-\gamma < \theta < -\beta$, the flow is assumed to be turbulent with a constant density ρ'. The main source of the turbulence is assumed to be the free surface, where there is breaking and dissipation of the short waves. Here we shall assume that the flow is so strongly turbulent that it is dominated by Reynolds stresses which can be represented by a constant eddy viscosity N, say. (This is a

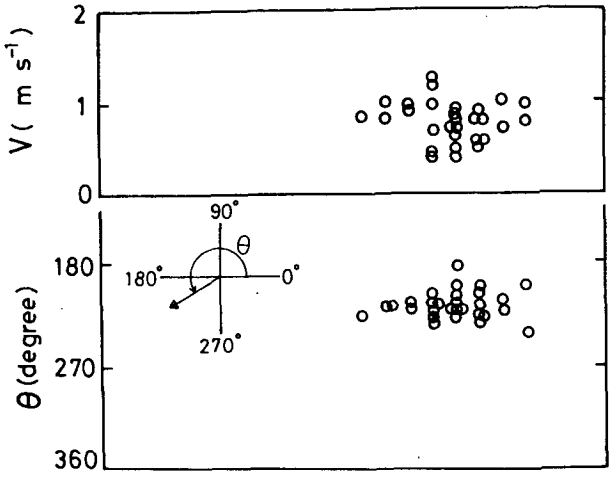

FIG. 2. Estimated velocities V and directions θ of the flow near the crest of wind waves, as calculated from observations of entrained bubbles. (From Koga 1982).

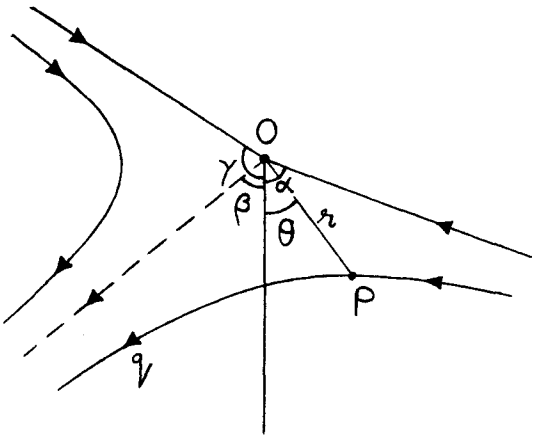

FIG. 3. Notation and coordinates for the theoretical model of section 2.

"turbulent Stokes flow" model). The streamfunction $\bar{\psi}$ for the mean flow then satisfies

$$\nabla^4\bar{\psi} = 0. \tag{2.5}$$

On the interface $\theta = -\beta$ we assume that

$$\bar{\psi} = 0 \tag{2.6}$$

so that there is negligible flow across the boundary, and the turbulent stresses are given by

$$P_{\theta\theta} = -p, \quad P_{r\theta} = C\rho q^2 \tag{2.7}$$

where p and q are given by Eq. (2.3) and (2.4), and C is a positive constant. We shall study in particular the case when C is small. (C is likely to be of the same order as the entrainment constant at the boundary of a turbulent jet, that is, of order 0.08; see Turner 1969). On the free surface $\theta = -\gamma$ we assume

$$\bar{\psi} = 0, \quad P_{\theta\theta} = 0, \quad P_{r\theta} = 0 \tag{2.8}$$

The above equations admit an exact solution in the form

$$\bar{\psi} = Er^3 \sin3(\theta + \gamma) + Fr^3 \sin(\theta + \gamma) \tag{2.9}$$

where E and F are constants. (For details see Longuet-Higgins 1973, sections 3 to 5). Some representative flows when $\rho = \rho'$ and $C > 0$ are shown in Fig. 4. The corner angle in the laminar flow to the right is always 120°. The angle of depression of the free surface lies between 0° and 11° (actually $\arctan 3^{-3/2}$, = 10°54′). The upwards inclination of the free surface in the flow to the left is supported by the turbulent Reynolds stresses.

The limit $C \to 0$ is of special interest. We find then that $F \to 0$ and so from (2.9)

$$\bar{\psi} = Er^3 \sin3(\theta + \gamma) \tag{2.10}$$

representing a simple, irrotational mean flow in a 60° corner. By symmetry, the tangential stress $P_{r\theta}$ vanishes both on the interface $\theta = -\beta$ and on the free surface $\theta = -\gamma$. The constant E is given by

$$E = 0.0156g/N \tag{2.11}$$

(see the Appendix to this paper).

The existence of the flow depends upon the eddy viscosity N being greater than zero. If N were replaced by the ordinary kinematic viscosity, then E would still be finite, but improbably large.

The above solution may be generalized to the case when $\rho'/\rho < 1$; see Longuet-Higgins (1973, section 5). In Figs. 9a and 9b of that paper the angles of inclination

$$\alpha' = 90° - \alpha, \quad \gamma' = \gamma - 90° \tag{2.12}$$

of the free surface on either side of the origin are shown as functions of the coefficient C. In the limiting case when $C \to 0$ both of the angles α' and γ' lie generally between 10°54′ and 30°.

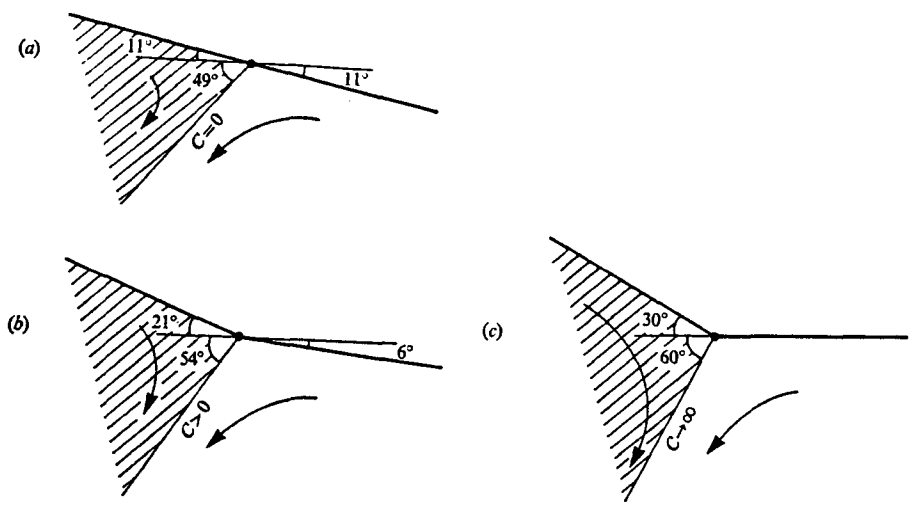

FIG. 4. (from Longuet-Higgins 1973). Examples of particular flows when $\rho = \rho'$ and $C > 0$. (a) $\delta = 60°$; (b) $\delta = 75°$; (c) $\delta = 90°$.

We may mention that when $\rho'/\rho < 1$ there exists a second class of solutions in which the flow velocity in the left-hand sector $-\gamma < \theta < -\beta$ is relatively small. Indeed when we let $C \to 0$ the fluid on the left becomes static. The inclination of the interface $\theta = -\beta$ is then given by

$$\tan\beta = (3\rho/\rho' - 1)/3^{1/2}. \qquad (2.13)$$

If $\rho'/\rho = 0$, we see that the configuration is that of the symmetric, 120° corner-flow. If on the other hand $\rho'/\rho = 1$, it is found that the flow velocity vanishes everywhere.

3. Comparison with observation

In Fig. 2b, which shows the direction of the flow as indicated by the bubble clusters (but allowing for the rate of rise of the bubbles relative to the surrounding fluid; see Koga 1982, section 2) the direction varies from 190° to 230°, i.e. 10° to 50° downwards from the horizontal, with a mean value 39°. This compares with the theoretical value 49° shown in Fig. 4 in the case $\rho' = \rho$, $C \to 0$. If we assume $\rho' < \rho$ the theoretical angle lies between 49° and 30°.

The magnitude of the velocities shown in Fig. 2a above range from 0.4 to 1.2 m s^{-1}, with a mean value 0.8 m s^{-1}. In the theoretical model the flow velocity q in the laminar region is given by equations (2.4) and (2.2), hence

$$q^2 = 2gr\cos\alpha. \qquad (3.1)$$

This depends both on r and α, but if as representative values we take $r = 0.05$ m, $\alpha = 39°$, we obtain $q = 0.87$ m s^{-1}, within the range of observation.

Consider now the inclination of the free surface. The photographs in Fig. 1 were taken from an angle slightly oblique to the line of the wave crests on the left. It can nevertheless be seen that the oblique line of bubbles separates from the surface at a point slightly forward of the wave crest. In Figs. 1a and 1c the crest profile is fairly sharply curved, so that the inclination of the tangent is not well defined. Nevertheless it can be seen that the oblique angle between the line of bubbles and the smooth part of the free surface ahead of the point of separation is not far from 120° as predicted by the theoretical model.

In Fig. 1b there appears to have been more than one separation event. The crest may also have become less steep since the earlier events. Nevertheless the angle between the lines of bubbles and the tangent to the mean surface is about 135°, only slightly greater than the predicted value.

From these comparisons we may conclude that there is a rough, but quantitative agreement between the observations and the predictions of the model.

4. Discussion

We emphasize first that the model of flow separation which has been suggested is only a local model, possibly applicable to the immediate neighbourhood of the point (or line) of separation. Like the Stokes 120° corner flow, it does not aim to describe the total flow in the wave, or even in the crest. Nevertheless a complete description of the flow must take into account the special conditions existing near the separation point, which may largely determine the global characteristics of the flow.

Perhaps the most controversial aspect of the model is its modeling of the turbulence by a uniform eddy viscosity. Such an assumption can be expected to yield, at best, only approximate, or qualitatively correct, predictions. Underlying the assumption is that the turbulence arises only partly from the shear layer along the boundary ($\theta = -\beta$) of the laminar flow. A much stronger source of turbulence is the dissipation of energy by short capillary-scale features near the wave crest. Such dissipation occurs naturally as a result of the breaking of capillary waves riding on the longer gravity waves. Such capillary waves are blocked by the gradients of velocity on the forward face of the gravity waves; see Phillips (1981). The turbulence so created will tend to be circulated by the mean flow in the turbulent sector of the fluid.

We have mentioned that the turbulence will help to support the inclination of the free surface to the left (i.e., up-wave) of the point of separation. In addition we may expect a contribution from the radiation stresses in the short capillary waves. The effect would be similar to the wave "set-up" maintained by waves in a coastal surf zone (Longuet-Higgins and Stewart 1963).

We note that Koga (1982) has proposed an explanation for the entrainment of bubbles at the point of separation. He suggested that it was analogous to the entrainment of air by a jet entering the surface from above. The presence of such jets is not evident in the photographs of Fig. 2. Rather, we believe the entrainment of air is to be associated with the stability of the flow near the point of separation. However the investigation of this problem is beyond the scope of the present paper.

5. Conclusions

Several features of the flow separation observed by Koga (1982) near the crests of steep gravity waves are in agreement with the simple theoretical model proposed earlier by Longuet-Higgins (1973). The latter assumes that on one side of the separating streamline the flow is irrotational, and on the other side it is turbulent. The turbulence, however, arises mainly from dissipation of energy at the free surface, and not from shearing at the separating streamline. The flow is essentially nonlinear, and is not contiguous to a state of rest. Aeration of the fluid by the entrainment of bubbles has only a small effect on the bulk density of the fluid.

A possible difference in density between the laminar

and turbulent regions has been included in the model in order to allow for the bulk effect of bubbles penetrating the free surface. However on the small scales considered here such density differences will probably be slight. Only in the case of large-scale spilling breakers where foaming is evident do we expect significant density differences (Longuet-Higgins and Turner 1974).

APPENDIX

The Evaluation of E and F

In section 3 of Longuet-Higgins (1973) it is shown that the boundary conditions (2.6) and (2.7) lead to the equations

$$\left.\begin{aligned} E\sin 3\delta + F\sin\delta &= 0 \\ E\sin 3\delta + \tfrac{1}{3}F\sin\delta &= -2CQ \end{aligned}\right\} \tag{A1}$$

and

$$E\cos 3\delta + F\cos\delta = -Q \tag{A2}$$

where

$$\delta = \gamma - \beta \tag{A3}$$

$$Q = \tfrac{1}{12}(g/N)\cos\left(\tfrac{2}{3}\pi - \beta\right). \tag{A4}$$

Hence

$$\cot 3\delta - \cot\delta = \frac{1}{3C} \tag{A5}$$

$$\csc 3\delta - \csc\delta = \frac{1}{3C}\,\frac{\cos\gamma}{\cos\left(\tfrac{2}{3}\pi - \gamma + \delta\right)}. \tag{A6}$$

We examine the solution as $C \to 0$ and $\delta \to \pi/3$. Writing

$$3C = \lambda, \quad \delta = \pi/3 + \delta', \tag{A7}$$

we find from (A5), to order ϵ^2, that

$$\frac{1}{3\epsilon} - \frac{1}{\sqrt{3}} + \frac{1}{3}\epsilon = \frac{1}{\lambda}. \tag{A8}$$

Now substituting into (A6) and expanding similarly in powers of ϵ we obtain

$$\left(1 + 2\sqrt{3} - \tfrac{1}{2}\epsilon^2\right)\cos(\gamma - \epsilon) = (1 - \sqrt{3}\epsilon + \epsilon^2)\cos\gamma \tag{A9}$$

whence to order ϵ^2

$$(3\sqrt{3}\epsilon - 2\epsilon^2)\cos\gamma + (\epsilon + 2\sqrt{3}\epsilon^2)\sin\gamma = 0. \tag{A10}$$

Assuming $\epsilon \neq 0$, we have, to lowest order

$$3\sqrt{3}\cos\gamma + \sin\gamma = 0 \tag{A11}$$

whence

$$\gamma = \tfrac{1}{2}\pi + \arctan 3^{-3/2} = 100°54'. \tag{A12}$$

We shall denote this value of γ by γ_0.

Now from equations (A1) we have

$$E = -\frac{3CQ}{\sin 3\delta} \sim \frac{\lambda Q}{3\epsilon} \sim Q \tag{A13}$$

$$F = \frac{3CQ}{\sin\delta} \sim \frac{\lambda\theta}{\sin\pi/3} \to 0 \tag{A14}$$

as $\epsilon \to 0$. Moreover from (A4)

$$\begin{aligned} Q &= \tfrac{1}{12}(g/N)\cos\left(\tfrac{2}{3}\pi + \delta - \gamma\right) \\ &\sim \tfrac{1}{12}(g/N)\cos(\pi - \gamma_0) \\ &= \tfrac{1}{12}(g/N)\sin(10°54'). \end{aligned} \tag{A15}$$

Hence the limiting value of E is

$$E_0 = Q = 0.0156(g/N) \tag{A16}$$

as stated in section 2.

REFERENCES

Banner, M. L., and O. M. Phillips, 1974: On the incipient breaking of small scale waves. *J. Fluid Mech.*, **65**, 647–656.

Crapper, G. D. 1957: An exact solution for progressive capillary waves of arbitrary amplitude. *J. Fluid Mech.*, **96**, 417–445.

Koga, M. 1982: Bubble entrainment in breaking wind waves. *Tellus*, **34**, 481–489.

Longuet-Higgins, M. S. 1973: A model of flow separation at a free surface. *J. Fluid Mech.*, **57**, 129–148.

——, 1987: Mechanics of wave breaking in deep water. *Proc. NATO Adv. Workshop on Natural Mechanisms of Surface Generated Noise in the Ocean*, Lerici, Italy, 15–19 June 1987.

——, 1989a: Monopole emission of sound by asymmetric bubble oscillations. I. Normal modes. *J. Fluid Mech.*, **201**, 525–541.

——, 1989b: Monopole emission of sound by asymmetric bubble oscillations. II. An initial-value problem. *J. Fluid Mech.*, **201**, 543–565.

——, and R. W. Stewart, 1963: A note on wave set-up. *J. Mar. Res.*, **21**, 4–10.

——, and J. S. Turner, 1974: An "entraining plume" model of a spilling breaker. *J. Fluid Mech.*, **63**, 1–20.

Phillips, O. M., 1981: The dispersion of short wavelets in the presence of a dominant wave. *J. Fluid Mech.*, **107**, 465–485.

Toba, Y., 1961: Drop production by bursting of air bubbles on the sea surface. III. Study by use of a wind flume. *Mem. Coll. Sci. Univ. Kyoto*, Ser. A, **29**, 313–344.

Turner, J. S., 1969: Buoyant plumes and thermals. *Ann. Rev. Fluid Dyn.*, **1**, 29–44.